

## Transonic buffet control by means of upper Gurney flaps

D'Aguanno, Alessandro; Schrijer, Ferdinand; van Oudheusden, Bas

**Publication date**

2019

**Document Version**

Accepted author manuscript

**Published in**

54th 3AF International Conference AERO2019 At: Paris, France

**Citation (APA)**

D'Aguanno, A., Schrijer, F., & van Oudheusden, B. (2019). Transonic buffet control by means of upper Gurney flaps. In *54th 3AF International Conference AERO2019 At: Paris, France* Article FP47-2019-daguanno

**Important note**

To cite this publication, please use the final published version (if applicable).  
Please check the document version above.

**Copyright**

Other than for strictly personal use, it is not permitted to download, forward or distribute the text or part of it, without the consent of the author(s) and/or copyright holder(s), unless the work is under an open content license such as Creative Commons.

**Takedown policy**

Please contact us and provide details if you believe this document breaches copyrights.  
We will remove access to the work immediately and investigate your claim.

# TRANSONIC BUFFET CONTROL BY MEANS OF UPPER GURNEY FLAPS

A. D'Aguanno<sup>(1)</sup>, F.F.J. Schrijer<sup>(2)</sup> and B.W. van Oudheusden<sup>(3)</sup>

Faculty of Aerospace Engineering, Delft University of Technology

Kluyverweg 2, 2629HS, Delft, The Netherlands

<sup>(1)</sup> A.Daguanno@tudelft.nl, <sup>(2)</sup> F.F.J.Schrijer@tudelft.nl, <sup>(3)</sup> B.W.vanOudheusden@tudelft.nl

## ABSTRACT

This study investigates the possibility of controlling transonic buffet by means of a Gurney Flap with an upward deflection at the trailing edge of the airfoil (UGF). Different geometries and dimensions of UGFs have been studied for their impact on the buffet behaviour. The effectiveness of the UGFs has been tested experimentally with Schlieren and PIV in the transonic-supersonic wind tunnel of TU Delft at  $Ma=0.7$ ,  $\alpha=3.5$ . It is found that the best performing UGF is a straight UGF with a height of 1.5% or 2% of the chord. These UGFs allow the reduction of the energy associated with buffet. This result has been corroborated by a flow description of the phases of buffet, a spectral analysis and a POD approach. In addition, the straight UGFs resulted to be effective in a less developed buffet condition too.

## 1. INTRODUCTION

Transonic buffet is one of the limiting factors for the flight envelope of a civil aircraft. It consists in the oscillation of a shockwave on the suction side of a wing, that takes place for a specific range of Mach Number, angle of attack and Reynolds Number ( $Ma$ ,  $\alpha$ ,  $Re$ ). In particular, the oscillation of the shock wave can lead to the structural oscillation of the wing (called buffeting). The first studies on transonic buffet have been carried out by *Lee* ([12]), who explained this phenomenon as the result of a feedback mechanism, in which the main elements are the shock movement and the presence of downstream and upstream travelling pressure waves. According to this model, the disturbances created at the shock foot travel downstream and reach the trailing edge (TE) and so are responsible for the formation of

other pressure waves. These waves travel upstream and interact with the shock, forcing it to move upstream or downstream according to the phase in which the downstream pressure waves are created; in this way the shock buffet mechanism is closed.

A different description of buffet from that of *Lee*, has been proposed by *Crouch* ([5],[6],[7]), who describes buffet as the result of a modal instability. The results of this stability analysis accurately predict the buffet onset for  $Ma$  and  $\alpha$ , and are in good agreement with the experimental data.

Updates to *Lee*'s feedback mechanism have been proposed by *Hartmann et al* [10], who consider vortex structures, which are shed in the separated area (and not at the shock foot), responsible for the formation of upstream travelling waves.

Because of the negative effects related with buffet, it is of paramount importance to either reduce or fully eliminate the phenomenon. In the paper of *Giannelis et al* [9] an overview of the main results achieved in controlling buffet are discussed, for both active and passive control systems, with higher precision and complexity associated to the former.

Various studies on the use of active control systems for controlling buffet have been conducted by *Onera*'s research group ([2],[3],[4],[8]), in particular using Trailing Edge Deflectors (TED), whose deflection is controlled (in a closed loop) by the unsteady measurements of the static pressure on the airfoil which is linked to the shock position and direction of movement.

When simplicity and reliability is preferred to precision, a passive control system can be used. The common working principle for the different kinds of passive control systems is to try to break the buffet feedback mechanism. This goal can be achieved either by acting

at the shock location, or in the trailing edge area, or in the separated area.

A first example of a passive control system is the Vortex Generator ([4]) which energizes the boundary layer, promoting attached flow and, therefore, inhibiting the shock induced separation. It is effective in reducing buffet and moving the buffet onset to higher angles of attack.

Another simple way of controlling buffet is achieved by using a Shock Control Bump (SCB), whose effect is described in detail by *Bruce et al* [1] and whose use for controlling buffet is discussed in [9], describing SCBs to be really effective only in the shock location and not in out of design conditions.

A further passive control system can be achieved using Trailing Edge Static Deflections ([8]); however, these have the negative effect of increasing the buffet onset for the lift coefficient but not for the angle of attack.

A particular form of Trailing Edge Static Deflection is a Gurney Flap, which is simply a fixed flap with a vertical deflection; it was first used for automotive applications and then started to be used in aeronautics with a downward deflection ([15],[18]), with the idea of increasing the pressure on the pressure side and increasing the circulation around the airfoil and, hence, the lift.

Alternatively, a Gurney Flap but then with an upward deflection can be used for reducing buffet, this approach has been numerically investigated by *Tian et al* [16],[17]. The results of [17] showed an increase of the buffet onset both for the angle of attack and for the lift coefficient when using an Upper Gurney Flap with a height of 1.5 % of the chord of the airfoil.

A solution that is present in literature for reducing the emission of pressure waves at the trailing edge is obtained by the use of serrated trailing edges, but, although their effectiveness has been confirmed for subsonic incompressible flows, there is still no investigation that validates their positive effect at transonic conditions [13].

## 2. EXPERIMENTAL INVESTIGATION

The current experimental investigation addresses the potential to control transonic buffet, using Upper Gurney Flaps (UGFs) mounted at the trailing edge of a supercritical airfoil. The use of UGFs is based on the possibility of reducing the oscillations of the shock wave by breaking the coherence of the formation of the upstream travelling waves at the trailing edge and, therefore, damaging the feedback mechanism. The effect of serration at transonic velocity has also been tested by using serrated UGFs. Different UGF shapes and heights have been selected in order to verify their effect. The three values of the height ( $h$ ) in relation to the chord of the airfoil ( $c$ ) are:

- 1.0 %  $c$ ;
- 1.5 %  $c$ ;
- 2.0 %  $c$ .

These values have been chosen in order to have the same order of magnitude as the height of the boundary layer. The height ( $h$ ) is considered in relation to the suction side of the airfoil at the trailing edge (which has a thickness  $t=0.075 \% c$ ). For each value of  $h$ , three different shapes of the UGFs were tested:

- a straight UGF;
- a wide serrated UGF;
- a narrow serrated UGF.

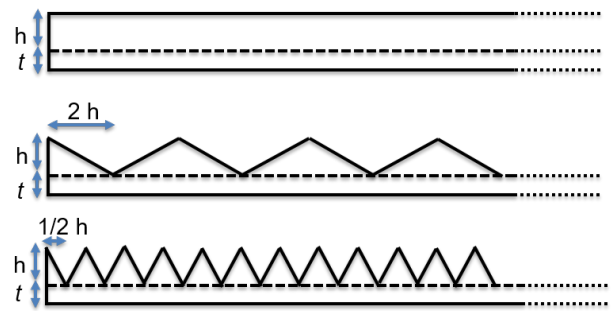


Figure 1: Shape of Upper Gurney Flaps, from the top to the bottom: straight, wide serration and narrow serration

As regards to serrated UGFs, the wide serration has a base of the sawtooth equal to two times  $h$ , while the narrow serrated UGF has the length of the base equal to  $0.5 h$ . A sketch of these UGFs is given in Fig. 1.

The motivation for using the serrated Upper Gurney Flaps is linked both to the aim of investigating their effect on the upstream travelling waves and to the desire of breaking the coherence of the buffet mechanism with a smaller reduction of lift in relation to the straight UGFs. In Fig. 2 a wide serrated UGF with a height of 2% of the chord can be seen mounted on the wind tunnel model.

The investigation that has been carried out is experimental and the tests have been performed in the transonic and supersonic blowdown wind tunnel of TU Delft, the TST 27, with a test section that is 270 mm high and 280 mm wide.

The airfoil used is the familiar supercritical OAT15A (designed by *ONERA*) with a span of 280 mm and a chord of 100 mm (Fig. 3). Furthermore, in order to ensure turbulent boundary layer, a transition trip has been applied at 7% of the chord of the airfoil.

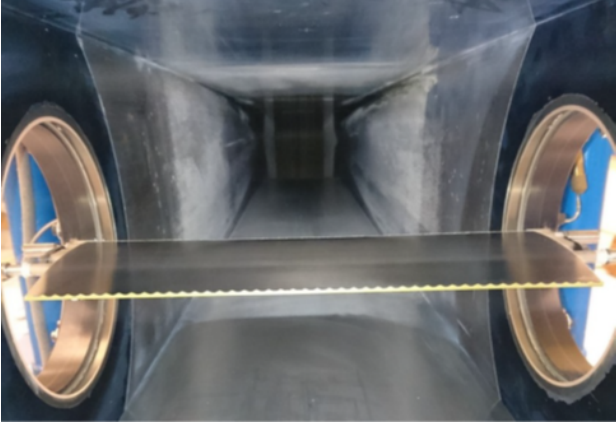


Figure 2: Example of an Upper Gurney Flap mounted on the OAT15A in the test section

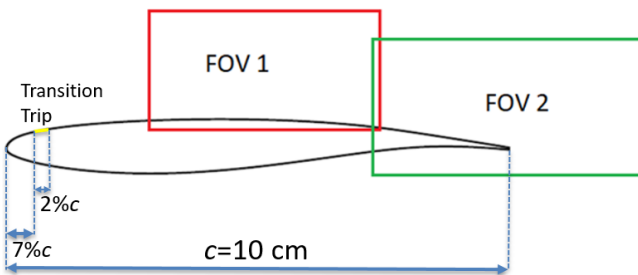


Figure 3: OAT15A airfoil and FOV PIV cameras

The experiments have been conducted with a free stream  $Ma=0.7$  and  $\alpha = 3.5$ , with a total pressure in the wind tunnel equal to 2 bars. In previous experiments that took place in the same wind tunnel on the same airfoil ([14]), buffet has been demonstrated to be fully developed for these conditions. In addition to this, a secondary buffet condition is studied ( $Ma=0.74$  and  $\alpha = 2.5$ ), in order to test the behaviour of the UGFs in an out-of-design condition.

High Speed Schlieren and Particle Image Velocimetry (PIV) have been applied in order to resolve the position of the shock in time.

The Schlieren investigation has been conducted with a conventional z configuration using a pinhole diameter of 2 mm, while the high speed camera Imager Pro has been used for acquiring images, with a resolution of 912\*816 pixels, exposure time of 15  $\mu s$  and a frequency of 5 KHz.

The set-up for High Speed PIV is shown in Fig. 4, where a high speed laser (Mesa Piv) and 2 Photron Fastcam SA-1 in 2C mode have been used. The two cameras acquire images at a frequency of 4650 Hz in double pulse mode ( $\Delta t=3\mu s$ ) with a resolution of 1024\*640 pixels. The two partially overlapping FOVs selected are shown in Fig. 3. As shown, the plane of interest is parallel to the chord of the airfoil, with the first FOV1 that covers an area extending from 30% of the chord to 80 % and FOV2

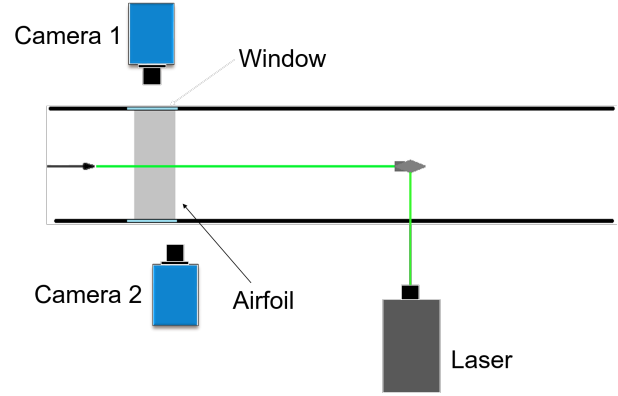


Figure 4: PIV set-up

that covers the area from 75% of chord to 125%, in order to also include the influences of the UGFs on the wake.

The data are processed in Davis (Version 8.4.0); first the reflections on the airfoil, are reduced by performing a time-minimum subtraction. Thereafter, by means of a cross correlation procedure, the velocity field is obtained. The cross correlation is computed with a multi-pass approach with 2 passes with a window size of 64 pixels and 2 passes with a final window size of 24 pixels; in both cases an overlap of 75% has been chosen with a vector spacing of 0.3% of the chord.

### 3. RESULTS

In order to describe the effects of the different UGFs in comparison to the clean configuration (No UGF), the results of the Schlieren campaign will be presented first and those of the PIV campaign subsequently. The results will be first discussed for  $Ma=0.7$  and  $\alpha=3.5$  and then for  $Ma=0.74$  and  $\alpha=2.5$

#### 3.1 Schlieren - Shock Dynamics

From the Schlieren visualization it is possible to obtain both a qualitative overview of the flow and a quantitative one (in terms of frequency and amplitude of the shock oscillation), thanks to the high speed recording. In Fig. 5 an instantaneous Schlieren image is shown underlining all the information that can be observed. In particular, it is possible to visualize the presence of a disturbance wave originating from the transition trip, the presence of the shock wave and the separated region that extends from the shock foot down to the trailing edge. Main differences in the use of UGFs in relation to the clean configuration (No UGF) can be both observed in the shape of the shock and at the TE. In fact, when using a straight UGF, some upwash appears at the TE; this

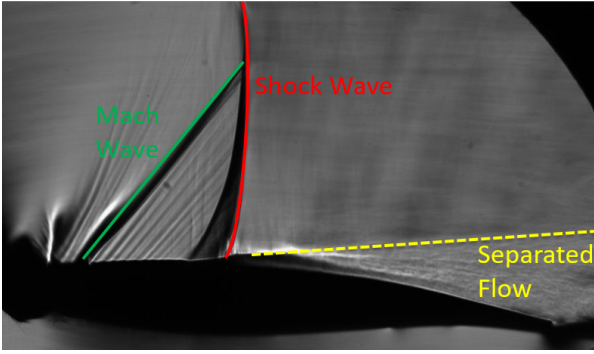


Figure 5: Main information obtained from a Schlieren image. The Mach wave is caused by the transition trip used.

behaviour is evident when the separated region reattaches (as shown in Fig. 6), but not during the upstream movement of the shock, when the separated area covers this effect completely. Moreover, it is interesting to note

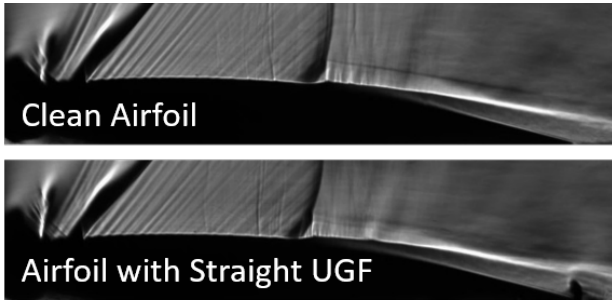


Figure 6: Detail of the upwash at the trailing edge for clean (top) and straight UGF (bottom) configuration

that, when using a serrated UGF, the shock is less well defined since with Schlieren the information is integrated along the span. From Fig. 7 it is clear that the area in which the shock is defined is wider than in the clean case, which supports the idea that the presence of UGFs does not have a negligible effect on the shock position and therefore on the whole buffet mechanism.

In order to further quantify this, the shock position has been tracked in time and used to perform a spectral analysis, from which the Power Spectral Density (PSD) associated to the shock position (in % of the chord) has been computed using the Welch method.

In Fig. 8 the pre-multiplied power spectrum has been plotted for the clean configuration, without any UGF, and for the configuration with a straight UGF with a height of 2% of the chord. It is clearly demonstrated that the main frequency of buffet remains at 160 Hz for this airfoil (as stated in [14]), which is also in good agreement in terms of Strouhal (St) number with the results obtained by *Jacquin et al* [11] for the same airfoil ( $St=0.067$ ).

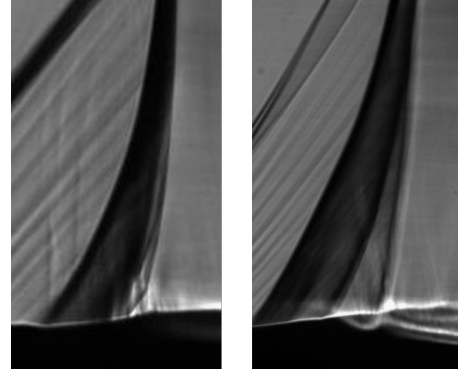


Figure 7: Detail of the shock structure for clean (left) and wide serrated UGF (right) configuration

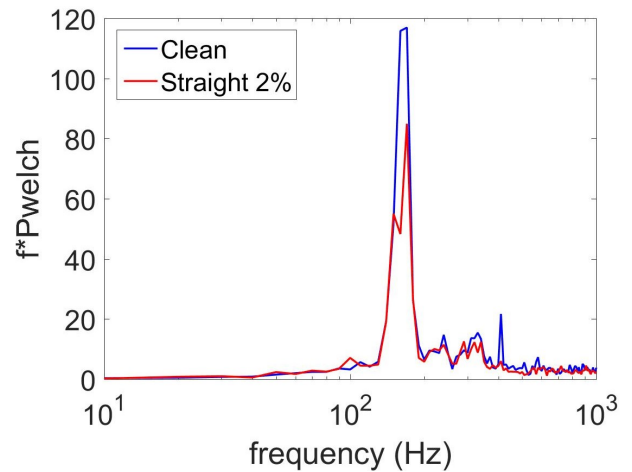


Figure 8: Pre-multiplied PSD related to the shock position

It is evident that when using an Upper Gurney Flap the frequency of motion of the shock is not affected, however the value of the main peak is clearly reduced without any apparent increase of energy for the secondary peaks. This observation seems to suggest that by using UGFs the feedback mechanism is not completely eliminated, but most likely only attenuated.

In order to further verify quantitatively if the energy associated with the shock oscillation is just rearranged or reduced, the pre-multiplied PSD is integrated in the frequency domain and plotted together with the value of the main peak at 160 Hz. The results of this investigation are shown in Fig. 9, for all of the configurations of the Upper Gurney Flaps, using the values for the clean airfoil as reference.

The first thing that stands out is that, for each configuration, the change of energy of the main peak corresponds to an almost proportional change of energy for the entire spectrum. It is evident that the use of the straight UGFs of 1.5% and 2.0% cause considerable reduction of energy associated with the shock oscillation, while the use

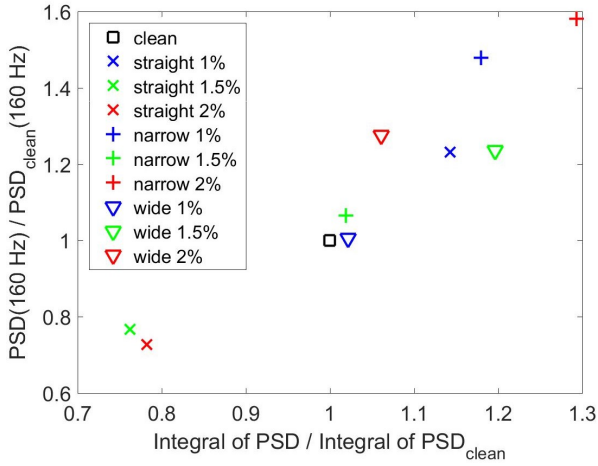


Figure 9: Integral in frequency of the PSD for all the configurations tested

of other UGFs (serrated) even lead to an increase of energy. This reduction of energy is already observable from the shock oscillation in time.

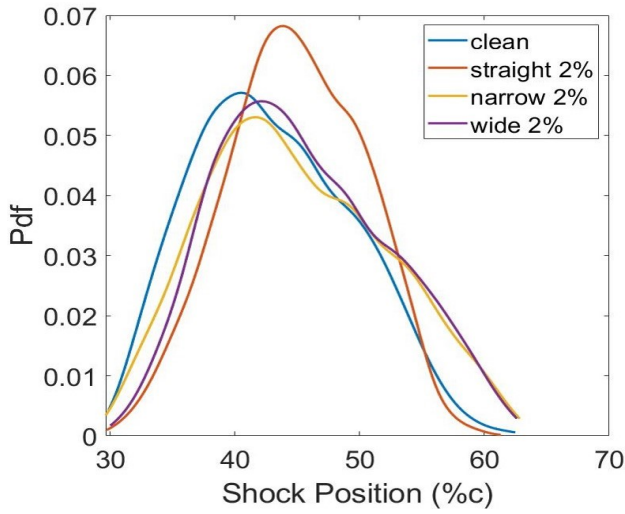


Figure 10: Probability Density Function of the shock position

To corroborate these results the probability density function of the shock position is shown in Fig. 10. From this plot what stands out is that the area in which the shock is likely to be found is much more limited for the straight 2%  $c$  UGF; as a consequence, there is a very distinct peak for the Pdf differently from what can be observed for the other configurations. Despite this, the average shock position does not change greatly for the different configurations and always remains between 40 and 45 % of the chord. It should be noted that, for the other configurations described in Fig. 10 (wide and

narrow UGF, both 2% $c$  high), there is no improvement in the range in which the shock oscillates.

## 3.2 Particle Image Velocimetry

In order to complement the results of the Schlieren measurements, more quantitative results were obtained with PIV.

The discussion of the results will be limited to the clean configuration and the one with the best performing UGF: the straight UGF with a height of 2% of the chord (straight 2% UGF). First a phase-averaged description of the flow field is given to properly characterize the buffet cycle.

### 3.2.1 Phase Average Flow Description

With the phase average a triple decomposition is used for the velocity:

$$u = u_{Avg} + u_{Phs} + u_{Turb} \quad (1)$$

So the velocity is described as the sum of a mean ( $u_{Avg}$ ), a periodic ( $u_{Phs}$ ) and a quasi-random fluctuating ( $u_{Turb}$ ) contribution. In the following figures the sum of the mean and the periodic contribution is plotted, and this represents the phase average. For the analysis the buffet cycle is divided into 8 phases according to the shock position and direction of its movement; with the first phase, the most upstream position is indicated, and with the fifth phase the most downstream one, as described in Fig. 11.

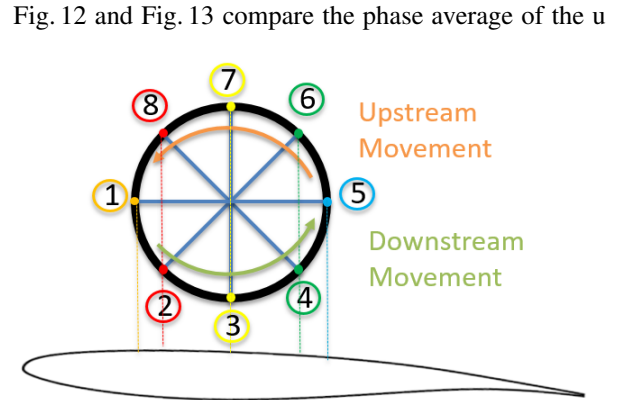


Figure 11: Phase Definition

component (horizontal) of the velocity for the clean and the straight UGF configurations. Results are plotted for the 1st (shock in the most upstream position) and the 5th phase (shock in the most downstream position). A first comparison highlights the differences in terms of amplitude of the oscillations, shape of the shock wave and of the separated area.

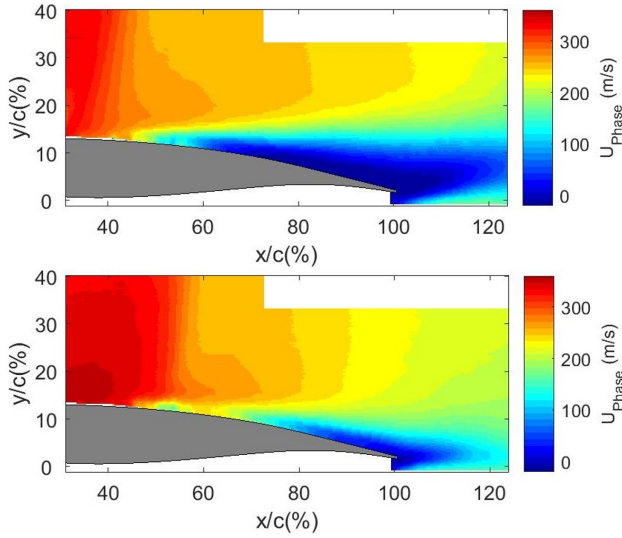


Figure 12: Phase average of the U component of the velocity for the clean configuration, with the shock in the most upstream position (1) (top figure) and downstream position (5) (bottom figure)

From these plots, it is evident that the amplitude of the oscillations of the shock is reduced when using a straight UGF compared to the clean configuration. This effect is confirmed by the fact that, for the straight UGF configuration in its most upstream position, the shock is around  $5\%c$  more downstream than in the clean configuration, while in the most downstream position it is  $5\%c$  more upstream.

This result is in good agreement with the probability density function for the shock position that has been discussed in the previous section (see Fig. 10).

In the most upstream position of the shock (phase 1), it can be furthermore observed that, for the clean configuration, the shock is more oblique and the separated area is more extended than for the straight UGF.

Since the shock is located more downstream in this phase, in presence of a UGF, higher values of the velocity are achieved for this configuration. The orientation of the shock can be verified by looking at the vertical component of the velocity, especially during the seventh phase, when the shock is halfway in its upstream travel. This phase is of particular interest because, throughout the cycle, the shock has here the highest relative velocity in relation to the flow, and with the associated compression bringing the strongest level of separation.

Fig. 14 presents the vertical component of the velocity for both the clean and the straight UGF configuration in the seventh phase. It is evident that the increase in vertical velocity at the shock foot is reduced when using a UGF. Besides, it is also clear that in the separated area the increase in vertical velocity is significantly higher when no UGFs are used. This results in a reduction in size of

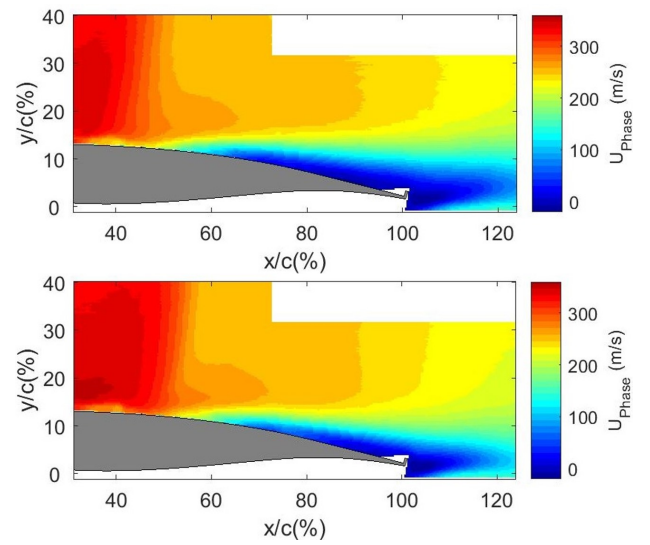


Figure 13: Phase average of the U component of the velocity for the straight ( $2\%c$ ) UGF configuration, with the shock in the most upstream position (1) (top figure) and downstream position (5) (bottom figure)

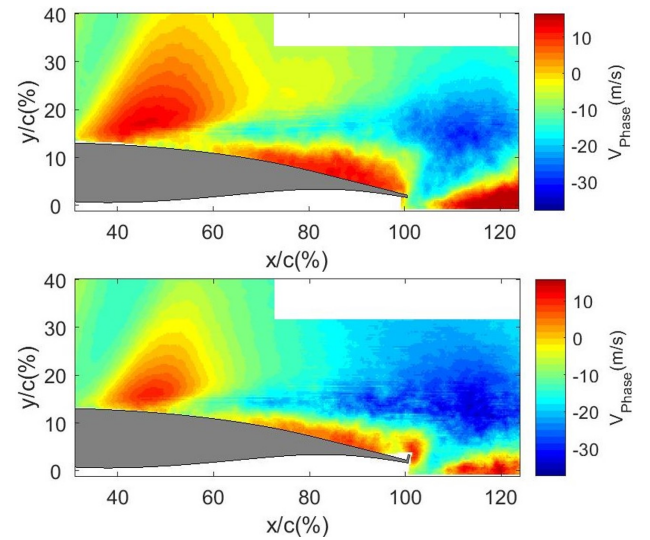


Figure 14: Phase average of the V component of the velocity for the clean configuration (top) and the straight one (bottom) with the shock in its upstream travel (7)

the separated area and therefore to a reduction of downstream pressure waves that are part of the transonic buffet mechanism.

It appears therefore that the effect of the Upper Gurney Flap at the trailing edge is that of decreasing the size of the separated area as predicted from the theory, thanks to the creation of vortices at the trailing edge and a net decrease of camber for the airfoil. The effect of the use of an upper flap at the trailing edge has been investigated by [17] through a numerical simulation and a typical result

is reported in Fig. 15. From this figure the presence of a clockwise vortex at the back of the flap and upwash behind the airfoil is predicted.

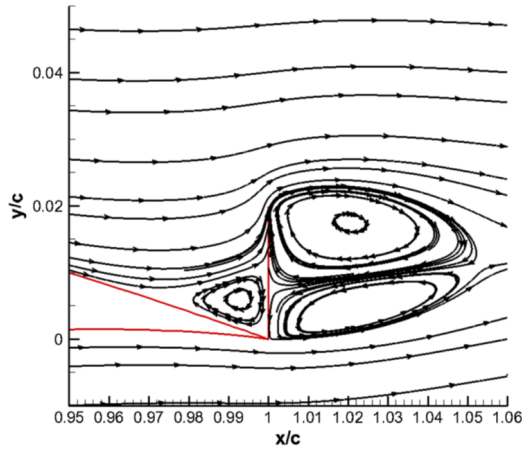


Figure 15: Streamline at the trailing edge of a RAE2822 airfoil [17]

### 3.2.2 Proper Orthogonal Decomposition

The unsteady aspects of the buffet mechanism have been further analyzed using POD (Proper Orthogonal Decomposition) on the fluctuating velocity fields.

With this decomposition the most energetic contributions, associated to the first eigenfunctions of the problem, can be obtained. Once the POD basis vector is obtained, a function (time coefficient), given by the projection of this base on the fluctuations of the velocity in time, is evaluated, and the power spectral density associated with the different modes is computed.

First of all the energetic contribution of the first modes are achieved and reported in Fig. 16, always for the clean and the straight UGF configuration.

In agreement with [14], it has also been found, with the present results, that in the clean case (No UGF) more than 80% of the total energy is associated to the the first three modes, which are related to different aspects of the buffet phenomenon. On the other hand, it is interesting to notice that when using the straight UGF a reduction of energy related to the first mode is achieved (of almost 10%), while for the secondary modes there is a slight distributed increase of energy.

This difference in the energy fraction confirms that the use of UGFs negatively affects the coherence of the buffet phenomenon, reducing the energy associated to the first mode (linked with buffet) and slightly increasing the energy associated with the secondary ones.

Comparing the first three modes for the two configurations, it should be noted that the physical meaning associated to the modes in presence of a straight UGF remains

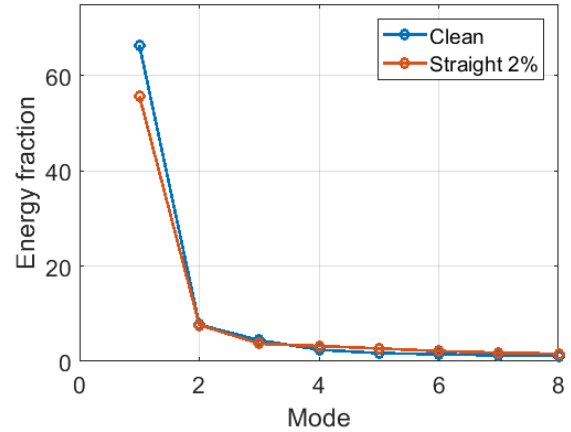


Figure 16: Comparison of the energy fraction associated to the different modes

the same as for the clean configuration. Therefore, in both cases, the first mode is associated with the oscillation of the shock position and with the concurrent thickening and reattaching of the separated area; the second and the third modes are related to the temporal asymmetry introduced by the unsteady behaviour of the shock motion and the separated area.

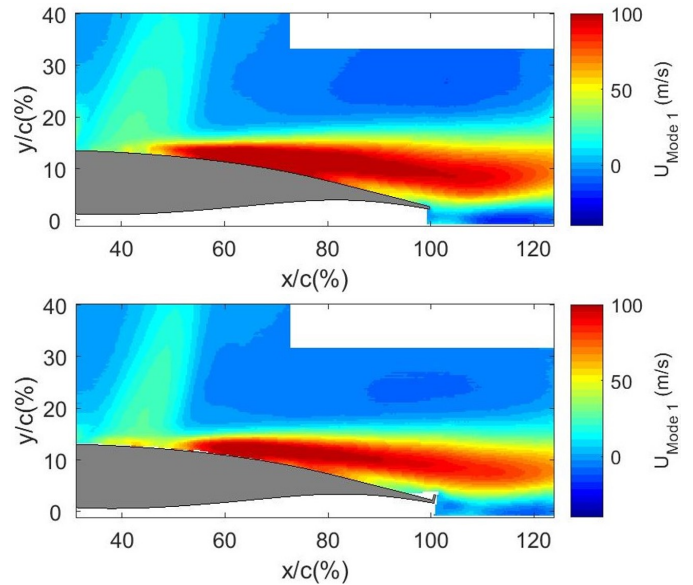


Figure 17: Comparison of the first mode shape for the U component for the clean (top) and the straight UGF configuration (bottom)

However, the largest differences between the two configurations are observed for the first mode, as shown in Fig. 17. For the clean case, the area in which the shock oscillates goes from 30% to 55% $c$ , whereas for the straight configuration from 35% to 50% $c$ , therefore,



for the clean configurations this area is wider. The same conclusions apply for the separated area which is wider in absence of any UGFs. Furthermore, for the straight UGF configuration, the area in which the oscillations relative to the separated flow are important, is moved downstream. No important differences are noted for the second and third modes, therefore, they are not considered any further (a more detailed description of these modes is given in [14]). Based on the time series of the POD coefficients, the power spectral density of the fluctuations in time associated to the different modes has been determined. In Fig. 18 the PSD for the first four modes of each of the configurations discussed is displayed.

First of all, it can be observed that, for both the configu-

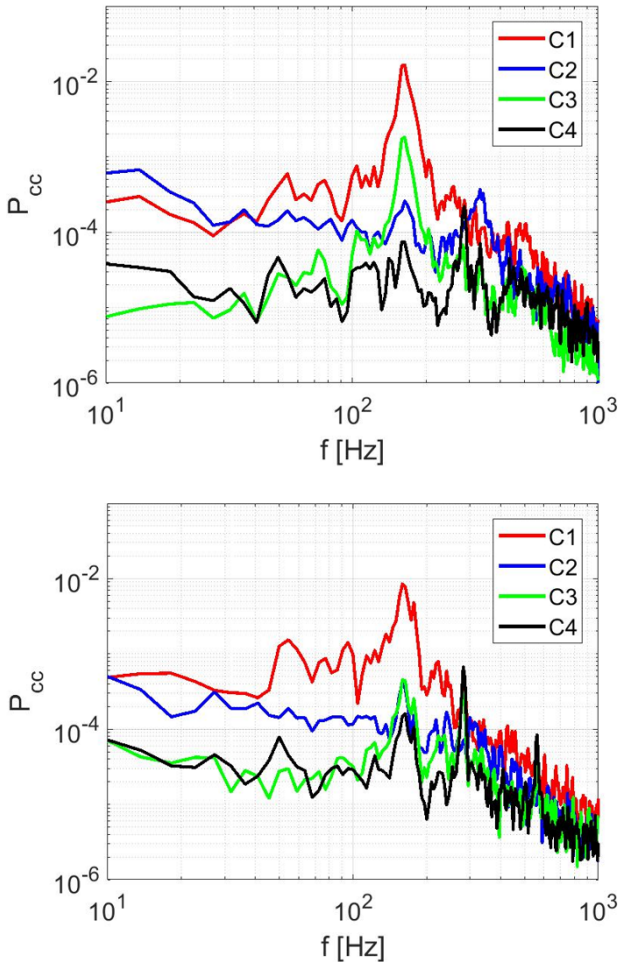


Figure 18: PSD associated to the first four modes for the clean (top) and the straight UGF configuration (bottom)

rations, the first 3 modes have a major contribution at the buffet frequency (160 Hz), while the fourth has an almost negligible contribution at that frequency. When using a UGF, the contribution of the first mode at the buffet frequency reduces clearly, but an even stronger reduction is obtained for the main peak of the third mode. On the

other hand, differently from the clean case, it seems that a more important role is played by the fourth mode, that has a secondary peak at 160 Hz and a primary one at a frequency that is double that of the buffet.

### 3.3 Off design buffet condition

As mentioned, a secondary buffet condition was investigated with  $Ma=0.74$  and  $\alpha=3.5$ , and the results discussed here are again limited to the clean and the straight UGF 2% configuration.

In Fig. 19 the energy fraction of the most energetic modes is plotted for both the configurations analyzed.

It is clear that in this case the energy associated to the first mode is lower than in the reference condition ( $Ma=0.7, \alpha=3.5$ ), which is included for reference as indicated by the dashed lines. Even in this condition the use

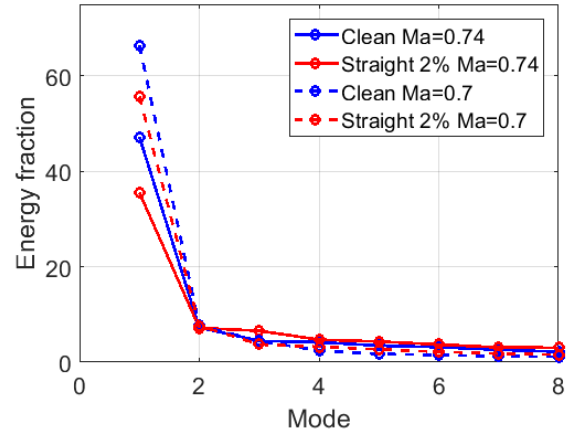


Figure 19: Comparison of the energy fraction associated to the different modes

of a straight UGF reduces the energy of the first mode (main contributor to buffet), energizing the secondary ones.

As previously done, the results for the PSD associated to the first four modes are discussed (Fig. 20). From these plots it is evident that for this condition the energy associated with buffet is lower than in the case of fully developed buffet, both for the clean and the straight configuration.

It is also interesting to point out that there is still a peak at 160 Hz, but for these conditions a higher peak appears at 400 Hz, which is associated with the facility characteristic frequency. All the modes have a contribution at this frequency, with the exception of the second mode.

The straight UGF configuration gives a reduction of energy for all the frequencies, except for the really low ones. At the buffet frequency (160 Hz), when using a straight UGF, a distinct single peak (as shown for the clean con-

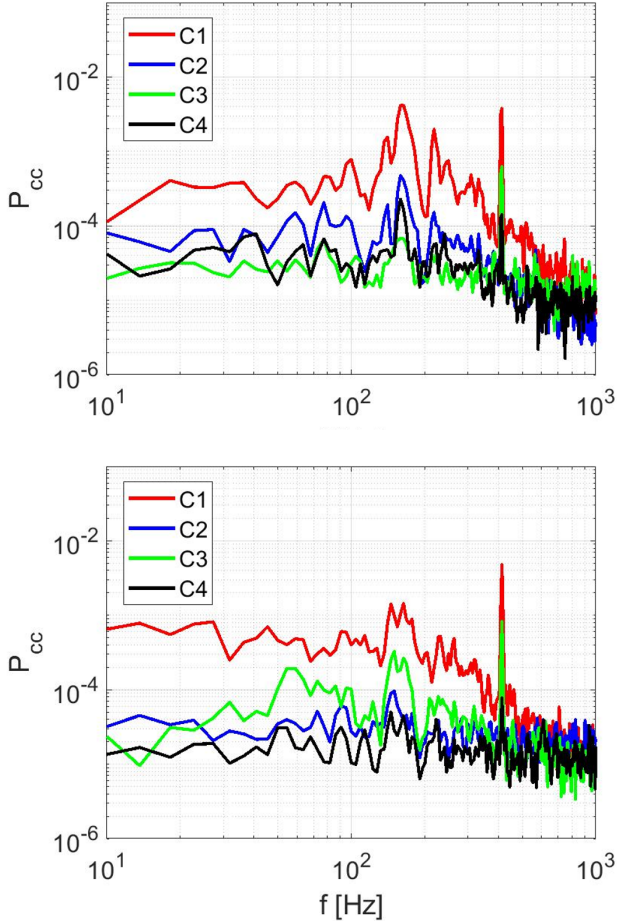


Figure 20: PSD associated to the first four modes at  $Ma=0.74$  for the clean (top) and the straight configuration (bottom)

figuration)no longer appears, demonstrating once again the capability of this UGF to break the buffet mechanism. Furthermore, for this flow condition it was observed that there is a reduction of the area in which the shock oscillates and of the separated area. This demonstrates that the straight UGF reduces the effect of buffet for this secondary condition too.

#### 4. CONCLUSIONS

In this paper the use of Upper Gurney Flaps for reducing transonic buffet on an OAT15A airfoil has been tested. The results showed a reduction of nearly 30% of the energy associated with buffet when using a straight UGF, with a height of 1.5% or 2% of the chord.

These results are in good agreement with [17], that is the only reference present in literature about the use of an Upper Gurney Flap and where a UGF with a height of 1.5% of the chord was found to be optimal in reducing buffet.

A spectral analysis has shown that the reduction of energy is achieved without changing the buffet characteristic frequency of the problem ( $St=0.067$ ), but just attenuating the peak of energy at this frequency. This reduction of energy results in a diminishing of the amplitude of oscillation of the shocks and of the separated area. These results are confirmed by both Schlieren and PIV measurements.

Thanks to the latter, the average flow field in different phases of the buffet cycle has been determined and they clearly demonstrate that the introduction of UGFs at the trailing edge (and the net increase of total camber of the airfoil) helped the separated area to reattach faster, thereby damaging the consistency of the transonic buffet mechanism. The decrease in camber should lead to a reduction in the lift coefficient, however, the numerical results obtained by [17] (with which this paper is in good agreement) showed an increase of the buffet onset both for the angle of attack and for the lift coefficient. To corroborate this theory, further investigation could be dedicated to the study of the formation of upstream travelling waves at the trailing edge when using UGFs and to the evaluation of buffet onset for the lift coefficient.

A POD analysis showed the most energetic modes that contribute to buffet. This has provided further understanding of one of the mechanisms by which buffet is attenuated with straight UGFs; in fact, with their use the total energy of the phenomenon is moved from the most energetic mode to the secondary ones. Despite this, no physical variation of the different modes occurs.

It should be pointed out that the best performing UGFs have a height of 1.5% and 2% of the chord, values that are close to the thickness of the boundary layer for this configuration. Therefore, the UGF with a height of 1% of the chord is not able to interact and disturb the feedback mechanism, achieving results similar to those for the clean shape.

The Schlieren images have shown how the use of serrated UGFs introduce 3D effects, having an effect on the shock location. Despite this, the use of serrated UGFs has proven to be ineffective and in some case they have even deteriorated buffet performances. This is in agreement with other results reported in literature concerning the use of serrated trailing edge at transonic velocities.

With the POD approach a second less developed buffet condition has been analyzed, showing a positive effect in the use of straight UGFs in this condition too, both for the buffet frequency and for secondary peaks that arise. This result is encouraging as most passive control systems present in literature are only effective in the design condition, but not in others.

## REFERENCES

- [1] P. J. K. Bruce and S. P. Colliss. Review of research into shock control bumps. *Shock Waves*, 25(5):451–471, Sep 2015.
- [2] D. Caruana, A. Mignosi, M. Corrège, A. Le Pourhiet, and A.M. Rodde. Buffet and buffeting control in transonic flow. *Aerospace Science and Technology*, 9(7):605 – 616, 2005.
- [3] D. Caruana, A. Mignosi, C. Robitailié, and M. Corrège. Active control of transonic buffet flow. *Flow, Turbulence and Combustion*, 824:312 – 351, 2003.
- [4] D. Caruana, A. Mignosi, C. Robitailié, and M. Corrège. Separated flow and buffeting control. *Flow, Turbulence and Combustion*, 71(1):221–245, March 2003.
- [5] J. D. Crouch, A. Garbaruk, D. Magidov, and L. Jacquin. Global structure of buffeting flow on transonic airfoils. In *IUTAM Symposium on Unsteady Separated Flows and their Control*, pages 297–306, 2009.
- [6] J. D. Crouch, A. Garbaruk, D. Magidov, and A. Travin. Origin of transonic buffet on aerofoils. *Journal of Fluid Mechanics*, 628:357 – 369, 2009.
- [7] J.D. Crouch, A. Garbaruk, and D. Magidov. Predicting the onset of flow unsteadiness based on global instability. *J. Comput. Phys.*, 224(2):924–940, June 2007.
- [8] C. Despre, D. Caruana, A. Mignosi, O. Reberga, and M. Correge. Buffet active control - experimental and numerical results. In *Proceedings of RTO AVT Symposium on Active Control Technology of Enhanced Performance Operational Capabilities of Military Aircraft, Land Vehicles, and Sea Vehicles*, 2001.
- [9] N.F. Giannelis, G.A. Vio, and O. Levinski. A review of recent developments in the understanding of transonic shock buffet. *Progress in Aerospace Sciences*, 92:39 – 84, 2017.
- [10] A. Hartmann and W. Feldhusen, A. and Schröder. On the interaction of shock waves and sound waves in transonic buffet flow. *Physics of Fluids*, 25(2):026101, 02 2013.
- [11] L. Jacquin, P. Molton, S. Deck, B. Maury, and D. Soulevant. Experimental study of shock oscillation over a transonic supercritical profile. *AIAA Journal*, 47(9):1985–1994, September 2009.
- [12] B. H. K. Lee. Transonic buffet on a supercritical aerofoil. *The Aeronautical Journal*, 1990.
- [13] J. M. Nies and H. Olivier. Dependence of upstream moving pressure waves on the mach number and the impact of trailing edge serrations. In *62. Deutscher Luft- und Raumfahrtkongress*, 2013.
- [14] F.F.J. Schrijer, R. Solana Perez, and B.W. van Oudheusden. Investigation of transonic buffet using high speed piv. In *Proceedings of the 5th International Conference on Experimental Fluid Mechanics (ICEFM 2018)*, 2018.
- [15] M. Suresh and N. Sitaram. Gurney flap applications for aerodynamic flow control. In *Proceedings of the 9th International Conference on Mechanical Engineering*, 2011.
- [16] Y. Tian, P. Feng, P. Liu, T. Hu, and Q. Qu. Spoiler upward deflection on transonic buffet control of supercritical airfoil and wing. *Journal of Aircraft*, 54(3):1229–1233, May 2017.
- [17] Y. Tian, Z. Li, and P. Q. Liu. Upper trailing-edge flap for transonic buffet control. *Journal of Aircraft*, 55(1):382–389, January 2018.
- [18] J. Wanga, Y. Lia, and K. Choi. Gurney flap -lift enhancement, mechanisms and applications. *Progress in Aerospace Sciences*, 35(12):1890–1891, 2008.